# Defying the disequilibrium:
## the usefulness of steady-state self-consistent models for the Galaxy

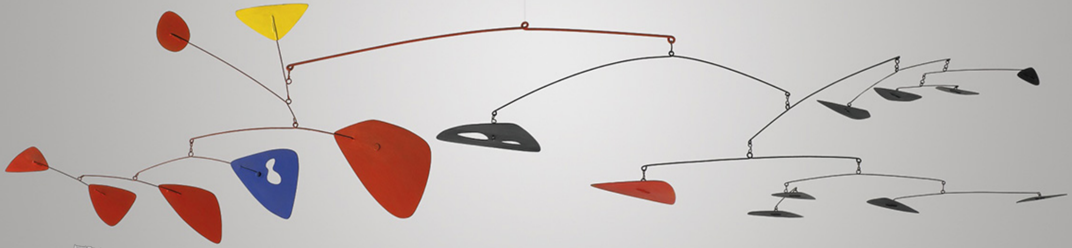


Milky Way

April 05, 2019

**Galaxy in crisis!**

The discovery of a new retrograde population in the Milky Way stellar halo shocked the entire astronomical community.

stars clearly trace a past accretion event, says an anonymous researcher at the Institute of Astronomy, Cambridge


Eugene Vasiliev

Institute of Astronomy, Cambridge


KITP, Santa Barbara, April 2019

# Why steady state?

Distribution function of stars $f(\mathbf{x}, \mathbf{v}, t)$
satisfies [sometimes] the collisionless Boltzmann equation:

$$\frac{\partial f(\mathbf{x}, \mathbf{v}, t)}{\partial t} + \mathbf{v}\,\frac{\partial f(\mathbf{x}, \mathbf{v}, t)}{\partial \mathbf{x}} - \frac{\partial \Phi(\mathbf{x}, t)}{\partial \mathbf{x}}\,\frac{\partial f(\mathbf{x}, \mathbf{v}, t)}{\partial \mathbf{v}} = 0.$$

# Why steady state?

Distribution function of stars $f(\mathbf{x}, \mathbf{v}, t)$
satisfies [sometimes] the collisionless Boltzmann equation:

$$\mathbf{v}\,\frac{\partial f(\mathbf{x},\mathbf{v})}{\partial \mathbf{x}} - \frac{\partial \Phi(\mathbf{x})}{\partial \mathbf{x}}\,\frac{\partial f(\mathbf{x},\mathbf{v})}{\partial \mathbf{v}} = 0.$$

3D

Steady-state assumption $\Longrightarrow$ Jeans theorem:

$$f(\mathbf{x}, \mathbf{v}) = f\left(\mathcal{I}(\mathbf{x}, \mathbf{v};\ \Phi)\right)$$

3D – 6D

integrals of motion ($\leq$ 3D?), e.g., $\mathcal{I} = \{E, L, \ldots\}$

# Initial conditions for perturbation analysis

Better start with an equilibrium configuration!

# Initial conditions for *N*-body simulations

Many of the commonly used methods for constructing initial conditions produce out-of-equilibrium systems and require an initial transient period to settle into a [different!] equilibrium configuration.

to ensure $Q_\star \geqslant 1.5$ everywhere. Since the initial conditions are for a system slightly out of equilibrium, each simulation was evolved for roughly 4 Gyr before being disturbed. We

[Bland-Hawthorn+ 2018]

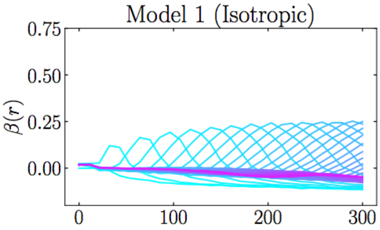


[Garavito-Camargo+ 2019]

This is not an unavoidable nuisance – shop for better methods!

# Holy Grail: the baseline model for the Milky Way

- no model is a perfect rendition of reality;
- the value of models is in their interpretability;
- makes sense to start with something relatively simple (equilibrium).

## Desirable features:

- distribution functions for individual chemically (and/or geometrically) distinct populations;
- dynamically self-consistent gravitational potential;
- flexibility of tuning and easiness of construction.

## No such models exist [yet?]

# Fundamental equations

distribution function

integrals of motion

gravitational potential

1. Collisionless Boltzmann equation:

$$\mathbf{v}\,\frac{\partial f}{\partial \mathbf{x}} - \frac{\partial \Phi}{\partial \mathbf{x}}\,\frac{\partial f}{\partial \mathbf{v}} = 0 \quad \Longrightarrow \quad f = f\big(\mathcal{I}(\mathbf{x}, \mathbf{v};\ \Phi)\big).$$

(Assumption: a galaxy is a collisionless system in a steady state)

2. Poisson equation:

total density

$$\nabla^2 \Phi(\mathbf{x}) = 4\pi\, G\, \rho(\mathbf{x}).$$

(Assumption: Newtonian gravity)

3. The link:

$$\rho(\mathbf{x}) = \iiint d^3v\, f(\mathbf{x}, \mathbf{v}).$$

(Assumption: self-consistency)

# Iterative approach

1. Assume a particular distribution function $f\left(\mathcal{I}\right)$;
2. Adopt an initial guess for $\Phi(\mathbf{x})$;
3. Establish the integrals of motion $\mathcal{I}(\mathbf{x},\mathbf{v})$ in this potential;
4. Compute the density $\rho(\mathbf{x}) = \iiint d^3v\; f\left(\mathcal{I}(\mathbf{x},\mathbf{v})\right)$;
5. Solve the Poisson equation to find the new potential $\Phi(\mathbf{x})$;
6. Repeat until convergence.

Origin: Prendergast & Tomer 1970;

used in Kuijken & Dubinski 1995, Widrow+ 2008, Taranu+ 2017 (GalactICs),

Piffl+ 2014, Cole & Binney 2016, Sanders & Evans 2016 (action-based formalism).

# How to compute the potential

1. Direct integration:

$$\Phi(\mathbf{x}) = -\iiint d^3x'\,\rho(\mathbf{x}') \times \frac{G}{|\mathbf{x}-\mathbf{x}'|}.$$

2. Azimuthal harmonic expansion:

$$\Phi(R,z,\phi) = \sum_{m=-\infty}^{\infty} \Phi_m(R,z)\,\mathrm{e}^{im\phi}.$$

interpolated functions

3. Spherical harmonic expansion:

$$\Phi(r,\theta,\phi) = \sum_{l=0}^{\infty}\sum_{m=-l}^{l} \Phi_{lm}(r)\,Y_l^m(\theta,\phi).$$

4. Basis-set expansion:

$$\Phi(r,\theta,\phi) = \sum_{n=0}^{\infty}\sum_{l=0}^{\infty}\sum_{m=-l}^{l} \Phi_{nlm}\,A_{nl}(r)\,Y_l^m(\theta,\phi).$$

(example: self-consistent field method of Hernquist&Ostriker 1992)

# How to compute the potential of a spheroidal system

**3.** Spherical-harmonic expansion:

$$\Phi(r,\theta,\phi) = \sum_{l=0}^{\infty} \sum_{m=-l}^{l} \Phi_{lm}(r)\, Y_l^m(\theta,\phi),$$

$$\Phi_{lm}(r) = -\frac{4\pi G}{2l+1}\left[ r^{-1-l}\int_0^r dr'\,\rho_{lm}(r')\,r'^{\,l+2} + r^l \int_r^{\infty} dr'\,\rho_{lm}(r')\,r'^{\,1-l}\right],$$

$$\rho_{lm}(r) = \int_0^{\pi} d\theta \int_0^{2\pi} d\phi\, \rho(r,\theta,\phi)\, Y_l^{m*}(\theta,\phi).$$

# How to compute the potential of a flattened system

**2.** Azimuthal-harmonic (Fourier) expansion:

$$\Phi(R,z,\phi) = \sum_{m=-\infty}^{\infty} \Phi_m(R,z)\,\mathrm{e}^{im\phi},$$

$$\rho_m(R,z) = \frac{1}{2\pi}\int_0^{2\pi} d\phi\ \rho(R,z,\phi)\mathrm{e}^{-im\phi},$$

$$\Phi_m(R,z) = -\iint dR'\,dz'\,\rho_m(R',z') \times \Xi_m(R,z,R',z'),$$

analytic expr. for Green's function:

$$\Xi_m(R,z,R',z') \equiv \int_0^{\infty} dk\ 2\pi G\ J_m(kR)\,J_m(kR')\,\exp(-k|z-z'|) =$$

$$= \frac{2\sqrt{\pi}\,\Gamma\left(m+\frac{1}{2}\right)\ {}_2F_1\left(\frac{3}{4}+\frac{m}{2},\ \frac{1}{4}+\frac{m}{2};\ m+1;\ \xi^{-2}\right)}{\sqrt{RR'}\ (2\xi)^{m+1/2}\,\Gamma(m+1)}$$

$$\text{where } \xi \equiv \frac{R^2+R'^2+(z-z')^2}{2RR'}.$$

# Gravitational potential extracted from N-body simulations

The spherical-harmonic and azimuthal-harmonic potential approximations can also be constructed from $N$-body models.

Advantages:
fast evaluation, smooth forces, suitable for orbit integration and analysis.

Real $N$-body model

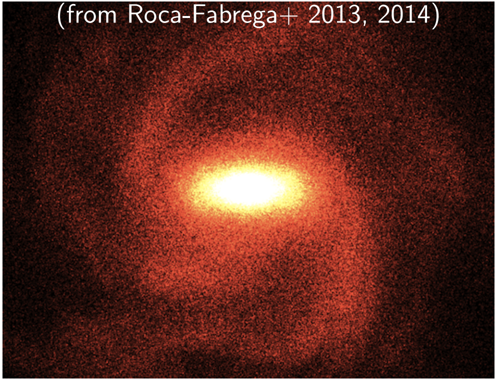


Potential approximation

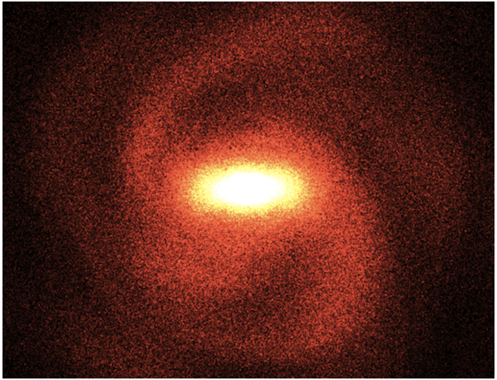

Work in progress: smooth potentials of FIRE simulations

# Actions as integrals of motion

One may use any set of integrals of motion, **but** actions are special:

$J = \frac{1}{2\pi} \oint \mathbf{p}\, d\mathbf{x}$, where $\mathbf{p}$ are canonically conjugate momenta for $\mathbf{x}$

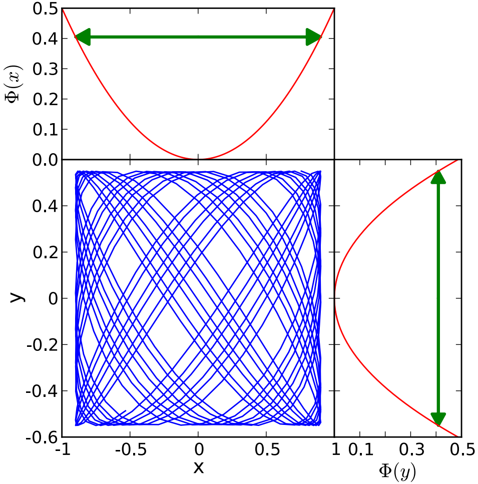


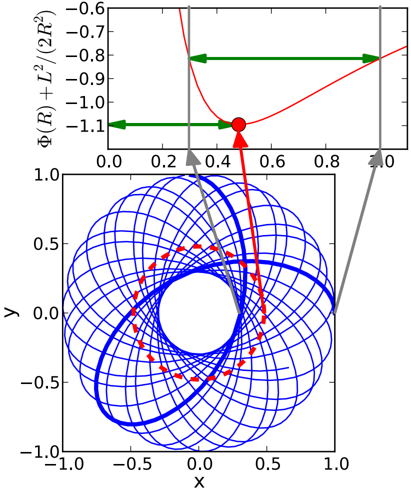

# Advantages of action/angle variables

- Clear physical meaning (describe the extent of oscillations in each dimension).
- Most natural description of motion (angles change linearly with time).
- Possible range for each action variable is $[0..\infty)$ or $(-\infty..\infty)$, independently of the other ones (unlike $E$ and $L$, say).
- Canonical coordinates $\Rightarrow$ total mass is computed trivially $M = \int f\big(\mathbf{x},\mathbf{v}\big)\; d^3x\; d^3v = \int f\big(\mathbf{J}\big)\; d^3J\; d^3\theta = \int f\big(\mathbf{J}\big)\; d^3J\;(2\pi)^3$, does not depend on $\Phi$, does not change between iterations.
- Actions are adiabatic invariants (are conserved under slow variation of potential) $\Rightarrow$ easy to construct multicomponent models.
- Serve as a good starting point in perturbation theory.
- Efficient methods for conversion between $\{\mathbf{x},\mathbf{v}\}$ and $\{\mathbf{J},\boldsymbol{\theta}\}$ exist (e.g., Stäckel fudge, Binney 2012, or Torus machine, Binney & McMillan 2016).

# "Classical" methods

- Spherical systems:
  two of the actions can be taken to be the *azimuthal action* $J_\phi \equiv L_z$ and the *latitudinal action* $J_\vartheta \equiv L - |L_z|$;
  the third one (the *radial action*) is given by a 1d quadrature:

  $$J_r = \frac{1}{\pi} \int_{r_{\rm min}}^{r_{\rm max}} dr \, \sqrt{2[E - \Phi(r)] - L^2/r^2},$$

  where $r_{\rm min}, r_{\rm max}$ are the peri- and apocentre radii.
  Angles are given by 1d quadratures. For special cases (the isochrone potential, and its limiting cases – Kepler and harmonic potentials), these integrals are computed analytically.
  Note: a related concept in celestial mechanics are the Delaunay variables.

- Flattened axisymmetric systems – the **epicyclic approximation**:
  motion close to the disk plane is nearly separable into the in-plane motion ($J_\phi$ and $J_r$ as in the spherical case) and the vertical oscillation with a fixed energy $E_z$ in a nearly harmonic potential ($J_z$).

# State of the art: Stäckel fudge

Fact: orbits in realistic axisymmetric galactic potentials are much better aligned with prolate spheroidal coordinates.

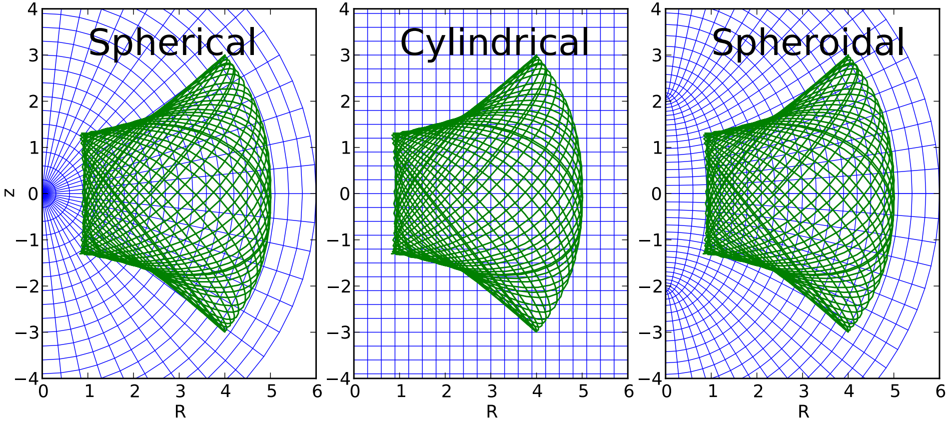

# State of the art: Stäckel fudge

Fact: orbits in realistic axisymmetric galactic potentials are much better aligned with prolate spheroidal coordinates.

One may explore the assumption that the motion is separable in these coordinates $(\lambda, \nu)$.

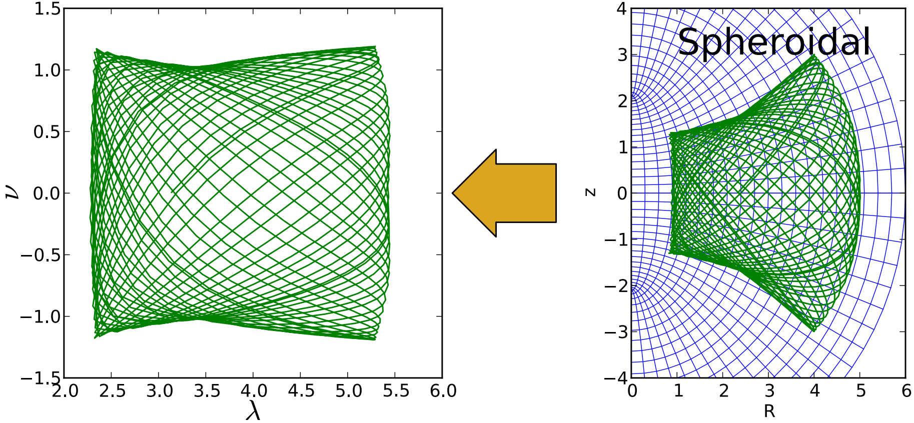

## Stäckel fudge [Binney 2012]

The most general form of potential that satisfies the separability condition is the Stäckel potential[1]: $\Phi(\lambda,\nu) = -\dfrac{f_1(\lambda) - f_2(\nu)}{\lambda - \nu}$.

The motion in $\lambda$ and $\nu$ directions, with canonical momenta $p_\lambda, p_\nu$, is governed by two separate equations:

$$2(\lambda - \Delta^2)\,\lambda\,p_\lambda^2 = \left[E - \frac{L_z^2}{2(\lambda - \Delta^2)}\right]\lambda - [I_3 + (\lambda - \nu)\Phi(\lambda,\nu)],$$
$$2(\nu - \Delta^2)\,\nu\,p_\nu^2 = \left[E - \frac{L_z^2}{2(\nu - \Delta^2)}\right]\nu - [I_3 + (\nu - \lambda)\Phi(\lambda,\nu)].$$

Under the approximation that the separation constant $I_3$ is indeed conserved along the orbit, actions are computed as

$$J_\lambda = \frac{1}{\pi}\int_{\lambda_\mathrm{min}}^{\lambda_\mathrm{max}} p_\lambda\,d\lambda, \quad J_\nu = \frac{1}{\pi}\int_{\nu_\mathrm{min}}^{\nu_\mathrm{max}} p_\nu\,d\nu.$$

[1] Note that the potential of the Perfect Ellipsoid [de Zeeuw 1985] is of the Stäckel form, but it is only one example of a much wider class of potentials.

# Stäckel fudge in practice

A rather flexible approximation: for each orbit, we have the freedom of using two functions $f_1(\lambda)$, $f_2(\nu)$ (directly evaluated from the actual potential $\Phi(R, z)$) to describe the motion in two independent directions. These functions are different for each orbit (implicitly depend on $E, L_z, I_3$). Moreover, we may choose the focal distance $\Delta$ of the auxiliary prolate spheroidal coordinate system for each orbit independently.

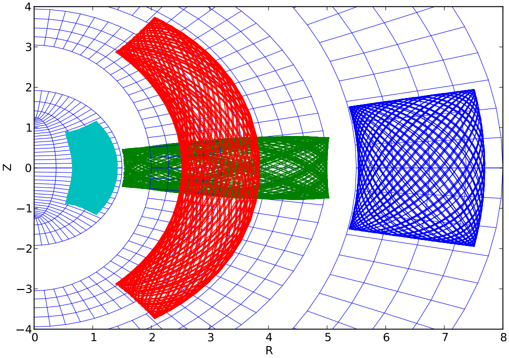

# Accuracy of the Stäckel fudge

Accuracy of action conservation using the Stäckel fudge: $\lesssim 1\%$ for most disk orbits, $\lesssim 10\%$ even for high-eccentricity orbits [except near resonances!].

Interpolation of $J_r, J_z$ on a 3d grid of $E, L_z, I_3$: 10x speed-up at the expense of a moderate [not always acceptable!] decrease in accuracy.

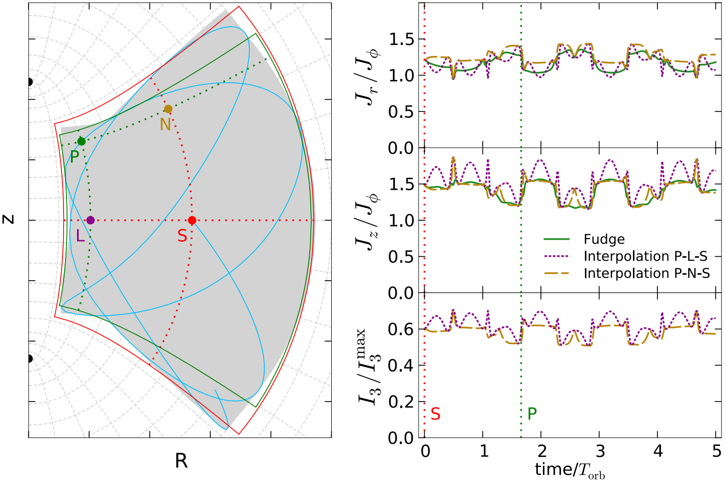

# Other methods for action computation

The accuracy of the Stäckel approximation is "uncontrollable" (cannot be systematically improved), and it is mainly used in axisymmetric potentials.

However, actions offer the only **systematic** method for computing the integrals of motion in a **non-perturbative** way for an arbitrary potential.

Canonical transformation between true $\{\mathbf{J}, \boldsymbol{\theta}\}$ and "toy" $\{\mathbf{J}^T, \boldsymbol{\theta}^T\}$ in some simple potential (e.g., isochrone), for which the mapping between position/velocity and action/angle coordinates is known (Torus construction – McGill&Binney 1990; McMillan&Binney 2008).

This transformation is described by a generating function $S(\mathbf{J}, \boldsymbol{\theta}^T)$, which can be expanded into Fourier series in $\boldsymbol{\theta}^T$; the accuracy of this approximation depends on the number of terms in the expansion.

A modification of this approach allows one to construct tori for resonantly-trapped orbits [Kaasalainen 1994; Binney 2016, 2018].

# Distribution functions in action space

- Spheroidal components (halo, bulge): double-power-law DF
  [Binney 2014, Posti+ 2015, Williams & Evans 2015]

$$f(\mathbf{J}) = \frac{M}{(2\pi\, J_0)^3} \left(\frac{h(\mathbf{J})}{J_0}\right)^{-\Gamma} \left[1 + \left(\frac{g(\mathbf{J})}{J_0}\right)^{\eta}\right]^{\frac{\Gamma-B}{\eta}} \exp\left[-\left(\frac{g(\mathbf{J})}{J_\mathrm{cut}}\right)^{\zeta}\right] \left(1 + \varkappa \tanh \frac{J_\phi}{J_{\phi,0}}\right),$$

$$g(\mathbf{J}) \equiv g_r J_r + g_z J_z + g_\phi |J_\phi|, \quad h(\mathbf{J}) \equiv h_r J_r + h_z J_z + h_\phi |J_\phi|$$

- Disk components: quasi-isothermal DF [Binney & McMillan 2011]

$$f(\mathbf{J}) = \frac{\tilde\Sigma\,\Omega}{2\pi^2\,\kappa^2} \times \frac{\kappa}{\tilde\sigma_r^2} \exp\left(-\frac{\kappa\, J_r}{\tilde\sigma_r^2}\right) \times \frac{\nu}{\tilde\sigma_z^2} \exp\left(-\frac{\nu\, J_z}{\tilde\sigma_z^2}\right) \times \begin{cases} 1 & \text{if } J_\phi \ge 0, \\ \exp\left(\frac{2\Omega\, J_\phi}{\tilde\sigma_r^2}\right) & \text{if } J_\phi < 0, \end{cases}$$

$$\tilde\Sigma(R_c) \equiv \Sigma_0 \exp\left(-\frac{R_c}{R_\mathrm{disk}}\right), \quad \tilde\sigma_r^2(R_c) \equiv \sigma_{r,0}^2 \exp\left(-\frac{2R_c}{R_{\sigma,r}}\right), \quad \tilde\sigma_z^2(R_c) \equiv 2\, h_\mathrm{disk}^2\, \nu^2(R_c).$$

- Alternative disk DF (exponential):

$$f(\mathbf{J}) = \frac{M}{(2\pi)^3} \frac{J}{J_{\phi,0}^2} \exp\left(-\frac{J}{J_{\phi,0}}\right) \times \frac{J}{J_{r,0}^2} \exp\left(-\frac{J\, J_r}{J_{r,0}^2}\right) \times \frac{J}{J_{z,0}^2} \exp\left(-\frac{J\, J_z}{J_{z,0}^2}\right) \times \begin{cases} 1 & \text{if } J_\phi \ge 0 \\ \exp\left(\frac{J\, J_\phi}{J_{r,0}^2}\right) & \end{cases}$$

# Construction of self-consistent models specified by DFs

Modelling procedure:

- Assume the parameters for the stellar and dark matter DFs
- Iteratively find the self-consistent potential/density corresponding to this DF:
  - Assume an initial guess for the potential
  - Initialize the action mapper for this potential
  - Recompute the density by integrating the DFs over velocity
  - Recompute the potential
- Compute the likelihood of the model given the data (compare the velocity distributions, microlensing depth, rotation curve)
- Adjust the parameters of the DFs

5 – 10 iter.

couple of minutes

The result: $\sim$ 15 parameters of DFs (mass, scale lengths and heights, velocity dispersions, etc.) and the final self-consistent potential as a by-product.

## Advantages of models based on distribution function

- Clear physical meaning
  (localized structures in the space of integrals of motion);
- Easy to compare different models
  (how to compare two $N$-body or $N$-orbit models?);
- Easy to compare models to discrete observational data;
- Easy to sample particles from the distribution function
  (convert to an $N$-body model);
- Stability analysis
  (perturbation theory most naturally formulated in terms of actions);

## Caveats:

- Implicitly rely on the integrability of the potential,
  ignore the presence of resonant orbit families (but see Binney 2016, 2018);
- So far implemented only for axisymmetric models
  (not a fundamental limitation).

# Perturbation theory in action space

$$
\begin{aligned}
f(\mathbf{J},\boldsymbol{\theta},t) &= f_0(\mathbf{J}) + \epsilon f_1(\mathbf{J},\boldsymbol{\theta},t),\\
H(\mathbf{J},\boldsymbol{\theta},t) &= H_0(\mathbf{J}) + \epsilon H_1(\mathbf{J},\boldsymbol{\theta},t) = H(\mathbf{x},\mathbf{v},t) \equiv \Phi_0(\mathbf{x}) + \epsilon\Phi_1(\mathbf{x},t) + \tfrac{1}{2}v^2.
\end{aligned}
$$

Linearized Vlasov / collisionless Boltzmann equation:

$$
0 = \frac{\partial f}{\partial t} + [H,f] \approx \frac{\partial f_1}{\partial t} + \frac{\partial f_1}{\partial \boldsymbol{\theta}}\frac{\partial H_0}{\partial \mathbf{J}} - \frac{\partial f_0}{\partial \mathbf{J}}\frac{\partial \Phi_1}{\partial \boldsymbol{\theta}}.
$$

$\Phi_1(\mathbf{x},t)$ is the external perturbation augmented with internal self-gravity (diverges at resonances!).

For the given $f_0$ and $\Phi_1$, one may compute the perturbed DF $f_1(\mathbf{J},\boldsymbol{\theta},t)$ [e.g., Monari+ 2016, 2017, 2018] – so far has only been done under epicyclic approximation, but a Stäckel generalization is possible.

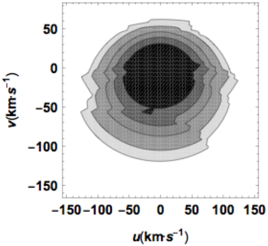

# Impact of disequilibrium on potential estimation

- Campbell+ 2017, Errani+ 2018: $\lesssim 10-20\%$ bias/scatter for a "sweet-spot" mass estimator (single number)
- Li+ 2016: $30-40\%$ scatter in M/L estimated by JAM models applied to a sample of Illustris galaxies
- Wang+ 2017: $20-50\%$ bias/scatter in halo mass/concentration estimated by spherical Jeans equation for APOSTLE simulations
- El-Badry+ 2017 "When the Jeans don't fit": $\sim 20\%$ bias in potential estimate from FIRE simulations
- Haines+ 2019: up to 50% overestimate of surface density estimated by 1d Jeans analysis applied to $N$-body simulations of Laporte et al.

Bottom line: steady-state assumption may substantially bias the results; need to calibrate your favourite method on realistic simulated data.

# AGAMA – All-purpose galaxy modeling architecture

- Extensive collection of gravitational potential models (analytic profiles, azimuthal- and spherical-harmonic expansions) constructed from smooth density profiles or $N$-body snapshots;
- Conversion to/from action/angle variables;
- Self-consistent multicomponent models with action-based DFs;
- Schwarzschild orbit-superposition models;
- Generation of initial conditions for $N$-body simulations;
- Various math tools: 1d,2d,3d spline interpolation, penalized spline fitting and density estimation, multidimensional sampling;
- Efficient and carefully designed C++ implementation, examples, Python and Fortran interfaces, plugins for Galpy, NEMO, AMUSE.

`arXiv:1802.08239`, `1802.08255`

`https://github.com/GalacticDynamics-Oxford/Agama`

# EQUILIBRIUM MODELS ARE USEFUL